Chaos transition despite linear stability

Thomas Gebhardt and Siegfried Grossmann
Fachbereich Physik der Philipps-Universität, Renthof 6, D 35032 Marburg, Germany
(Received 26 April 1994; revised manuscript received 22 June 1994)

We present a linearly stable model in two complex dimensions that can be triggered by an initial perturbation or external noise to exhibit chaotic dynamics although all linear perturbations are damped. The transition to chaos is caused by an interplay between transient linear growth and nonlinear, energy conserving mixing. The linear growth mechanism is due to the non-normality of the linearized dynamics in the vicinity of the stationary point. We consider this combined mechanism of non-normal growth and nonlinear mixing as a model for a new but often realized transition scenario from laminar flow to turbulence.

PACS number(s): 47.27.Cn, 47.20.−k, 03.40.Gc

I. INTRODUCTION

Linear stability can coexist with complicated dynamic behavior. This seems obvious since outside the basin of attraction of a stable fixed point the structure of the phase space may be rather intricate. Less obvious is the fact that the basin of attraction can be much smaller than the range of validity of the linearizable dynamics. This can happen if trajectories starting in the linear vicinity of the fixed point can transiently leave the linearizable range although all eigenvalues have a negative real part. If the nonlinear terms are then taken into account in addition, these trajectories can even escape the vicinity of the fixed point completely. Recent papers [1–5] suggest that such a scenario of linear transient growth combined with proper nonlinear mixing may take place in linearly stable shear flows which nevertheless become turbulent. It may also be relevant in other cases with asymptotically stable dynamics, e.g., in Ginzburg-Landau-type equations.

Mathematically the transient linear growth is a characteristic feature if the linearized dynamics is non-normal, i.e., if it does not commute with its Hermitian conjugate. While the importance of non-normality as a transient linear growth mechanism has recently already been discussed by various authors [1–5], here we emphasize the complementary action of the nonlinear mode mixing. Although the nonlinearity does not feed energy into the system, it can prevent the dissipative decay reflected by the negative real parts of the eigenvalues by redistributing the available energy to those modes which are able to gain energy transiently. We shall show that the proper combination of transient growth and nonlinear mixing is able to permanently balance the energy loss and the energy gain on a finite level, even if the initial disturbance is orders of magnitudes smaller. The level of this balance is, of course, in the range of influence of the nonlinearities and therefore the time evolution can be chaotic or turbulent.

II. MODEL

We present a simple system of ordinary differential equations (ODE's) that will follow the outlined route. Our notation is oriented on hydrodynamical terminology although we do not model a particular flow problem. Clearly we need at least two real variables to enable non-normality. Such a two-variable model has been considered including nonlinear mixing already in [4]. At least three (real) variables are necessary to allow chaotic motion in an autonomous system. Since the nonlinear dynamics shall be conservative, we chose to take four real or equivalently two complex variables u_1 and u_2, each representing the amplitude and the phase of some flow pattern. These flow patterns are imagined to be eigenmodes of a fluid flow in the absence of some background shear flow (typically denoted as Stokes modes). The whole flow consists of a supposedly stable laminar shear flow $\mathbf{U}_0$ plus some deviation $\delta\mathbf{u}$. This latter one is thought to be expanded in terms of the Stokes mode patterns. Thus $\mathbf{u}(t) := [u_1(t); u_2(t)]$ has the meaning of the amplitude vector of a deviation $\delta\mathbf{u}$ of the flow field from a linearly stable shear profile $\mathbf{U}_0$.

Our model equation for $\mathbf{u}(t)$ is

$$\dot{\mathbf{u}}(t) = (A_1 + \mathcal{R}A_2)\mathbf{u} + B(\mathbf{u},\mathbf{u}) + \mathcal{R}C(\sigma||\mathbf{u}||)\mathbf{u}. \quad (1)$$

Let us specify this equation term by term. First of all, $A_1\mathbf{u}$ describes the linear decay of the eigenmodes in the absence of the laminar background flow. The decay rates are determined in real flow by the geometry of the boundaries and the viscosity of the fluid. They define a typical viscous time scale. Another time scale which is dynamical is given as the ratio of a typical length of the system to the typical velocity of the laminar flow field. We have chosen to nondimensionalize the velocity by the viscous time scale. Then the dynamical time scale is just the inverse Reynolds number $\mathcal{R}^{-1}$, i.e., $\mathcal{R}$ measures the velocity of the basic flow $\sim \mathbf{U}_0$ in terms of the viscous velocity. This is close to the experimental situation where the boundaries and the viscosity are kept fixed, but the mean velocity of the fluid and thus $\mathcal{R}$ is varied. One must keep in mind, however, that in this gauge a fixed nondimensional time corresponds to more and more "revolutions" of the flow field if one increases the velocity of the fluid and thus the Reynolds number. To model all this we take A_1 to be a diagonal matrix with entries -18 and -38, independent of the Reynolds number $\mathcal{R}$, which mimics the

decay rates of the two eigenmodes. These decay rates reflect the result of the Laplacian in the Navier-Stokes equation, which means that they are of the order of a few $-\pi^2$ for the least stable eigenmodes. The additional linear term $\mathcal{R}A_2\mathbf{u}$ describes the influence of the laminar shear flow background $\mathbf{U}_0$ on $\delta\mathbf{u}$. We decompose

$$A_2 := \gamma A_{2c} + A_{2n}$$

$$\text{where} \quad A_{2c} := \begin{pmatrix} 0.8i & 0 \\ 0 & 1.1i \end{pmatrix}, \quad A_{2n} := \begin{pmatrix} 0 & 0.7 \\ 0 & 0 \end{pmatrix}, \tag{2}$$

again in close resemblance to actual flow field matrix elements. A_{2c} reflects the convective effect of the background flow on the eigenmodes and is therefore purely imaginary. It originates from the term $(\mathbf{U}_0 \cdot \boldsymbol{\nabla})\delta\mathbf{u}$ in the linearized Navier-Stokes equation. This convection effect depends on the orientation of the eigenmodes relative to the shear profile. It vanishes ($\gamma = 0$) for modes that do not vary in streamwise direction. The choice $\gamma = 1$ or $\gamma = 0$ will enable us to investigate the influence of the convection on the behavior of the flow. The term A_{2n} corresponds to $(\delta\mathbf{u}\cdot\boldsymbol{\nabla})\mathbf{U}_0$ in the linearized Navier-Stokes equation. It is responsible for the non-normality of the system and allows the transfer of energy from the background flow $\mathbf{U}_0$ into the perturbation $\delta\mathbf{u}$. The specific numbers for the matrix elements are chosen to mimic the gradient, i.e., a factor of π, the mean shear velocity, i.e., a factor of $\mathcal{R}/2$, and the orthogonal projection.

Next, the term $B(\mathbf{u},\mathbf{u})$ in the evolution equation (1) models the nonlinear interaction $(\delta\mathbf{u}\cdot\boldsymbol{\nabla})\delta\mathbf{u}$ between different perturbations. In accordance with the Navier-Stokes equation we demand it to be conservative and quadratic in $\mathbf{u}$. Conservative means that it will not change the total "energy" $\mathbf{u}^*\cdot\mathbf{u}$ of the perturbation, but just redistributes it among the different modes. The latter requirement deserves a comment. In highly symmetric geometries, where the eigenmodes are, e.g., plane waves, the eigenspaces can be classified by the conserved components of their wave vectors. Eigenspaces with different wave vectors are orthogonal of course. Thus the non-normality of the linearized Navier-Stokes dynamics can act only *within* each such subspace. Since the Navier-Stokes nonlinearity $(\mathbf{u}\cdot\boldsymbol{\nabla})\mathbf{u}$ does not couple directly, eigenmodes within the same subspace due to momentum conservation, non-normality, and second-order nonlinear interaction do not combine. In generic geometries there will, however, be no such selection rules and the linear modes will interact directly, giving rise to a quadratic term in the evolution equation. We shall regard such a situation and take $B =: (B_1, B_2)$ of the form

$$\begin{aligned} B_1(\mathbf{u},\mathbf{u}) &= b_1u_1u_2 + b_2u_1u_2^* + b_3u_1^*u_2 + b_4u_1^*u_2^* \\ &\quad -b_7^*u_2^2 - (b_5^*+b_6)u_2u_2^* - b_8u_2^{*2}\,, \\ B_2(\mathbf{u},\mathbf{u}) &= b_5u_1u_2 + b_6u_1^*u_2 + b_7u_1u_2^* + b_8u_1^*u_2^* \\ &\quad -b_3^*u_1^2 - (b_1^*+b_2)u_1u_1^* - b_4u_1^{*2}\,. \end{aligned} \tag{3}$$

The parameters $b_1, b_2, \ldots, b_8$ reflect the different wave numbers of the modes and some geometrical prefactors. The ansatz (3) conserves energy for any choice of $b_1,\ldots,b_8$. We will use the set $b_1 = 0.2$, $b_2 = 0.4i$, $b_3 = 0.6$, $b_4 = 0.8i$, $b_5 = 1.0$, $b_6 = 1.2i$, $b_7 = 1.4$, and $b_8 = 1.6i$. These b values are in a range of the high-dimensional parameter space where the dynamics exhibits chaotic attractors, depending, of course, on $\mathcal{R}$. There are other parameter ranges (not even far away) which lead to limit cycle solutions. Since we want to mimic the transition to turbulence in a driven flow field, we prefer the choice of the system parameters that leads to a chaotic behavior. But the underlying dynamical mechanism, namely, the interplay between non-normality and nonlinear interaction in a linearly stable system, is also vivid in parameter ranges where our model asymptotically leads to a limit cycle.

We have not yet accounted for some property of the Navier-Stokes equation. The energy of the perturbations may increase temporarily, but nevertheless it remains globally bounded. (For a rigorous prove of this statement in the case of plane Couette flow see [6].) We now argue the following: If the perturbations grow, they will tend to flatten the original shear profile $\mathbf{U}_0$ and thus inhibit further growth of the perturbation energy. Such a mechanism has not yet been implemented by the A and B terms on the right-hand side of (1). Indeed, depending on the Reynolds number $\mathcal{R}$, the actual choice of the b_i, and the initial conditions, the energy happens to grow infinitely in the numerical solutions. To inhibit that we added the third term

$$C(\sigma||\mathbf{u}||) := -\frac{\sigma||\mathbf{u}||}{1+\sigma||\mathbf{u}||}\,A_{2n}, \tag{4}$$

which in effect implements this feedback mechanism by switching off the non-normality when $||\mathbf{u}|| = (u_1u_1^* + u_2u_2^*)^{1/2}$ becomes large. σ is a real parameter that determines the size of $||\mathbf{u}||$ for which the feedback will become significant. We take $\sigma := 10/\mathcal{R}$; then further growth will be squeezed if $||\mathbf{u}||$ reaches a size which is somewhat less than the order of $||\mathbf{U}_0|| \sim \mathcal{R}$, reflecting the fact that the fluctuations in turbulent fluids are typically somewhat smaller in magnitude than the background flow. This completes the definition of our dynamical model.

III. NON-NORMALITY

Let us consider first the linear properties of the model. Obviously the eigenvalues of $A := A_1 + \mathcal{R}\,A_2$ are $\lambda_1 := -18 + 0.8\gamma\mathcal{R}\,i$ and $\lambda_2 := -38 + 1.1\gamma\mathcal{R}\,i$. In particular the real parts of λ_1 and λ_2 are independent of the Reynolds number. The first eigenvector $\mathbf{v}_1 = [1;0]$ is also independent of $\mathcal{R}$, but the second one (not normalized) varies, $\mathbf{v}_2 = [-7\mathcal{R}/(200-3\gamma\mathcal{R}\,i);1]$. For nonzero $\mathcal{R}$ the two eigenvectors are no longer orthogonal, indicating non-normality of A. This deviation from being orthogonal can be measured by $a = |\mathbf{v}_1^*\times\mathbf{v}_2|/(||\mathbf{v}_1||\,||\mathbf{v}_2||)$, which is shown in Fig. 1. A second effect of non-normality is the sensitivity to perturbations. This can be quantified by the ϵ pseudospectrum. The ϵ pseudospectrum of the matrix A is defined as the set in the complex λ plane $P(\epsilon) := \{\lambda \mid 1/(||(A-\lambda)^{-1}||_2 \le \epsilon\}$. For each $\lambda \in P(\epsilon)$

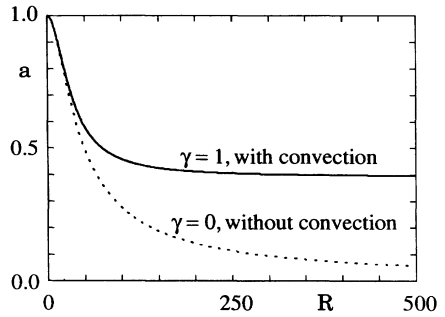

FIG. 1. Area a spanned by the normalized eigenvectors of A as a function of the Reynolds number $\mathcal{R}$. The dashed curve decreases asymptotically $\sim 1/\mathcal{R}$.

there is a perturbation A_{pert} such that λ is an eigenvalue of $A + A_{\text{pert}}$. The ϵ pseudospectrum of a non-normal system covers a substantially larger area in the complex frequency plane around the eigenvalues than that of a normal system. This means that in non-normal systems small perturbations can result in large modifications of the spectrum. We asked for the smallest norm ϵ_{min} of all perturbations A_{pert} that will shift the first eigenvalue λ_1 of A from $-18 + 0.8\gamma\mathcal{R}\,i$ to $0.8\gamma\mathcal{R}\,i$, i.e., such that $A + A_{\text{pert}}$ becomes marginally stable. This ϵ_{min} depends of course on $\mathcal{R}$. It is given by $\epsilon(\mathcal{R}, 0.8\gamma\mathcal{R}\,i)$, where $\epsilon(\mathcal{R}, \lambda) := 1/[||(A(\mathcal{R}) - \lambda)^{-1}||_2]$. For normal operators A, ϵ_{min} would be exactly the distance of λ to the nearest eigenvalue, which would result in 18 in our model. ϵ_{min} is shown in Fig. 2. The pseudospectrum is relevant also in a related context, namely, in resonant amplification of external noise. The response amplitude of a linear system excited externally with a frequency ω is determined by the norm of the resolvent $\epsilon^{-1}(\mathcal{R}, i\omega) = ||(A(\mathcal{R}) - i\omega)^{-1}||_2$. Hence a large pseudospectrum also implicates resonant amplification of external excitation with frequencies that are far away from the eigenfrequencies of the system ("pseudoresonance"). As visible in both Figs. 1 and 2, there are remarkable differences between the convective case $\gamma = 1$ and the nonconvective case $\gamma = 0$. For $\gamma = 1$ the effects of non-normality saturate at Reynolds numbers of a few hundred when $\mathcal{R}\,A_2$ dominates A_1. Then both the diagonal and the nondiagonal elements of A scale with $\mathcal{R}$, so that their ratio, which is responsible for the degree of non-normality, saturates. As an elementary calculation shows, the level of saturation depends

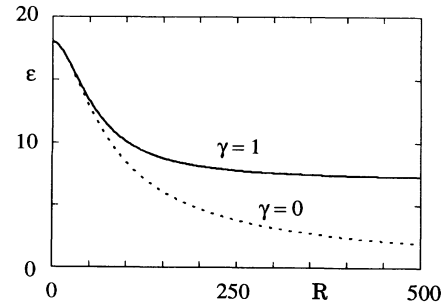

FIG. 2. ϵ_{min} as a function of the Reynolds number $\mathcal{R}$.

on the *difference* of the diagonal elements of γA_{2c}, more general on the eigenvalue difference. In terms of the hydrodynamical point of view this can be understood by the following argument. If the streamwise velocity of the two localized mode patterns are different (which may be due to the different location of their amplitude maximums relative to the background profile), then the time in which their amplitudes do overlap will shrink with increasing $\mathcal{R}$. This limits the non-normality.

This effect can indeed be observed in the behavior of hydrodynamical systems. In plane Couette flow there are pseudoresonances $\epsilon^{-1}(\mathcal{R}, i\omega)$ that grow like $O(\mathcal{R})$ [4], but only for small ω. We expect the modes which give rise to this growth to have large wavelengths in streamwise direction and thus no significant drift. For large ω there is no such growth of $\epsilon^{-1}(\mathcal{R}, i\omega)$ with $\mathcal{R}$, indicating the absence of modes with a common drift velocity corresponding to that large ω. In Ref. [7] the influence of white noise on plane Poiseuille flow is reported. Here too one can observe that the effect of non-normal amplification is most enhanced for modes with large wavelengths in streamwise direction.

In actual flow fields more and more modes get involved in the dynamics if the Reynolds number is increased. We consider this as the reason for the fast (exponential) decrease of the volume spanned by the linear eigenvectors of pipe flow perturbations, observed in Ref. [1]. Of course, our model cannot reproduce this feature.

Non-normal linear systems allow transient energy amplification even if their spectrum would suggest pure damping. The time evolution of the energy is determined by $A^\dagger + A$ (in our notation). $A^\dagger + A$ is Hermitian and has a positive eigenvalue for $\mathcal{R} > 74.72$ for both choices of γ in A_2, thus allowing transient energy growth. The mechanism for this transient energy amplification is the different time evolution of different eigenmodes. Consider a perturbation that is almost perpendicular to all eigenmodes. This has to be represented by a superposition of eigenvectors with rather large amplitudes that balance to a moderate sum, namely, the size of the disturbance. If this balance of the superposition is destroyed in the course of time due to the different corresponding eigenvalues, the perturbation energy will grow transiently even if each individual eigenmode contribution decreases. Hence one might expect that the transient energy growth is more enhanced for the convective case $\gamma = 1$ than for the nonconvective $\gamma = 0$ case, because in the former case the decorrelation takes place more rapidly. This effect is, however, superseded by the counterbalancing tendency of the degeneration of eigenmodes which does not saturate with increasing $\mathcal{R}$ in the latter case. As a result, the maximum energy amplification factor α is always larger for $\gamma = 0$ than for $\gamma = 1$ as we have outlined in Fig. 3. The maximum energy is reached either at the dynamical time scale (for $\gamma = 1$) or at the viscous time scale (for $\gamma = 0$). Figures 3(c) and 3(d) show two typical evolutions of the perturbation energy together with $||e^{A^\dagger t} e^{At}||_2$, which constitutes an upper bound on the normalized perturbation energy $[\mathbf{u}^*(t) \cdot \mathbf{u}(t)]/[\mathbf{u}^*(t=0) \cdot \mathbf{u}(t=0)]$. The oscillations resemble some kind of Poincaré recurrence property and

would disappear if one would allow more degrees of freedom.

Transient amplification requires Reynolds numbers above a certain threshold. This can be defined by that $\mathcal{R}_0$ above which $\alpha > 1$. In our model that happens at $\mathcal{R}_0 = 74.72$. But even if one is beyond threshold $\mathcal{R} > \mathcal{R}_0$, whether amplification occurs depends on the kind of perturbation. Clearly, initial disturbances in the direction of the A eigenvectors always immediately decay. But initial disturbances whose direction is nearly orthogonal to the A eigenvectors enjoy transient enhancement. The amplification is all the better the more the disturbance "misfits" the eigendirections. These misfit disturbances are thus the ones that can draw energy from the basic laminar flow, which is responsible for the non-normality and thus enables the misfit.

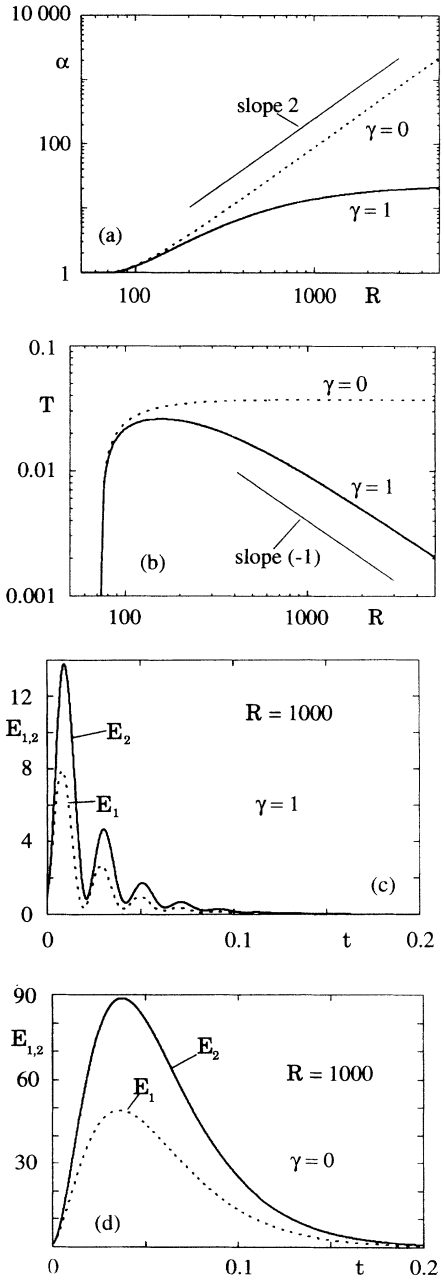

FIG. 3. (a) Maximum energy amplification factor α. (b) Time T to reach maximum of energy. (c) Energy bound $E_2 = ||e^{A^\dagger t} e^{At}||_2$ (solid line) and energy $E_1 = ||\mathbf{u}(t)||^2$ (dashed line) of the system $\dot{\mathbf{u}} = A\mathbf{u}$ starting with $\mathbf{u}(t=0) = [1;1]/\sqrt{2}$. γ is 1. (d) Same as (c), but for $\gamma = 0$.

IV. NONLINEAR MIXING

Now we include the nonlinear parts of Eq. (1). Without the nonlinear terms any perturbation will eventually fade away, even if there is transient amplification. This follows from the negative real parts of the A eigenvalues. Any disturbance is rotated eventually in the A eigendirection and then decays. The role of the nonlinearity is to reestablish misfitted components again by the interactions among the modes that constitute the amplified initial disturbance. Parts of the available energy are thus used to produce again a misfit disturbance that can draw energy once more; the other part of the energy is dissipated immediately. This energy redistribution happens permanently, so permanently misfitted amplitudes are present and permanently energy is drawn from the basic flow via non-normality, permanently balancing the dissipative loss. Since the interaction B depends on the details of the energy distribution over the $\mathbf{u}$ components, this redistribution process is quite complicated and chaotic, but self-sustaining.

The attractor of the nonlinear temporal evolution depends on the actual choice of the parameters in B and on the initial conditions. It may be a fixed point, a limit cycle, quasiperiodic or chaotic. In our model (1) the attractor numerically [8] turns out to be more irregular for $\gamma = 1$ than for $\gamma = 0$ since the advective case $\gamma = 1$ brings in two more frequencies. Nevertheless, there are common qualitative features of the model that are independent of the specific choice of the B parameters. We describe these generic features now. If the Reynolds number is too small, each initial perturbation will die out ("relaminarize"). As mentioned above, the threshold value for energy amplification is $\mathcal{R}_0 = 74.72$. The actual transition to turbulent behavior due to the self-sustaining feedback mechanism occurs if $\mathcal{R}$ is about an order of magnitude larger than $\mathcal{R}_0$ and depends on the initial disturbance. The onset of turbulence happens at generally lower $\mathcal{R}$ for $\gamma = 0$ than for $\gamma = 1$. We demonstrate this in Fig. 4. Even if the Reynolds number is large enough, the system will return to the fixed point $\mathbf{u} = \mathbf{0}$ if the initial amplitude is too small because the nonlinear feedback (which is quadratic in $\mathbf{u}$) is not strong enough to compensate the asymptotic exponential decay of the linear system. Since both the energy amplification factor and the corresponding time scale are larger without advection ($\gamma = 0$) than with advection ($\gamma = 1$), the initial amplitude, which is sufficient to produce "turbulence," is much smaller in the former case; cf. Fig. 5.

In order to investigate this turbulence transition in detail we calculated the temporal evolution for differ-

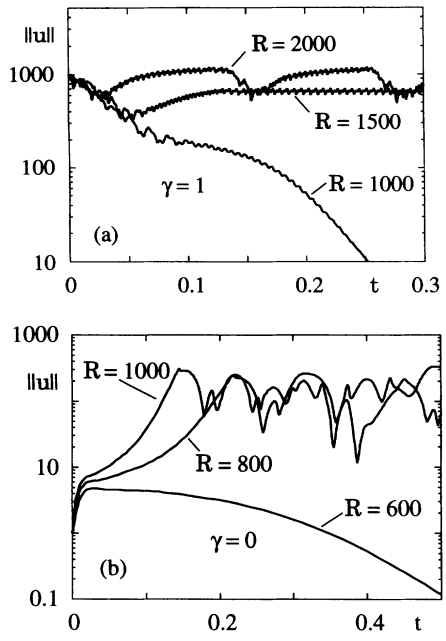

FIG. 4. (a) Perturbation amplitude $||\mathbf{u}(t)||$ for the model equation (1) and different Reynolds numbers. The initial vector is $\mathbf{u}(0) = [0; 1\,000]$; advection is included. (b) Same as in (a), but without advection. The initial vector is $\mathbf{u}(0) = [0; 1]$ here and the Reynolds numbers are lower than in (a).

ent Reynolds numbers and various initial amplitudes. In Fig. 6 we plotted the resulting amplitude $||\mathbf{u}(t)||$ at $t = 0.5$ as a function of both $\mathcal{R}$ and $||\mathbf{u}(0)||$. For each value $||\mathbf{u}(0)||$ of the initial amplitude we averaged over a randomly chosen ensemble of ten different realizations $\mathbf{u}(0)$. As can be seen in the diagram, the threshold initial amplitude $||\mathbf{u}(0)||_{\text{thr}}$, which is necessary to escape the laminar fixed point and to establish the turbulent state, shrinks with increasing Reynolds numbers if we take $\gamma = 0$ (nonadvective case), while it remains constant or even increases if we take advection into account, $\gamma = 1$. The reason for this behavior is, of course, that the non-normality increases with increasing Reynolds number for the nonadvective case whereas it asymptotically remains constant for $\gamma = 1$.

The energy $E = ||\mathbf{u}||^2/2$ satisfies the balance equation

$$\frac{dE(t)}{dt} = [\mathbf{u}^* A_1 \mathbf{u} + \mathcal{R}\mathbf{u}^*(A_2 + C)\mathbf{u}]_{\text{real part}} . \qquad (5)$$

The nonlinearity $B(\mathbf{u}, \mathbf{u})$ does not contribute. The first term on the right-hand side describes the dissipation, the second one the input rate. Figure 7 shows the temporal behavior of these contributions to the energy balance. While the dissipation rate $D = -18|u_1|^2 - 38|u_2|^2$ is in phase with and roughly proportional to the energy itself, the non-normal term fluctuates strongly:

$$\dot{E}_{\text{in}} = (u_1^* u_2 + u_2^* u_1)_{\text{real part}}\, 0.7\mathcal{R}/(1 + \sigma||\mathbf{u}||) \qquad (6)$$

originates from the interaction of the disturbance with the laminar background flow. It can be both, positive or negative, i.e., energy feeding or drawing. In the time average $\langle \dot{E}_{\text{in}} \rangle$ is positive and precisely balances $\langle D \rangle$.

If advection is allowed, the degree of non-normality saturates, $\sigma||\mathbf{u}|| = O(1)$, i.e., $||\mathbf{u}|| \propto \mathcal{R}$. Then $(u_1^* u_2 + u_2^* u_1)/||\mathbf{u}||^2$ is of the order $1/\mathcal{R}$. Without advection, there is no saturation of the non-normality, i.e., $\sigma||\mathbf{u}||$ exceeds 1. Then $(u_1^* u_2 + u_2^* u_1)/||\mathbf{u}||^2$ is of the order of 1 and thus $||\mathbf{u}|| \propto \mathcal{R}^2$.

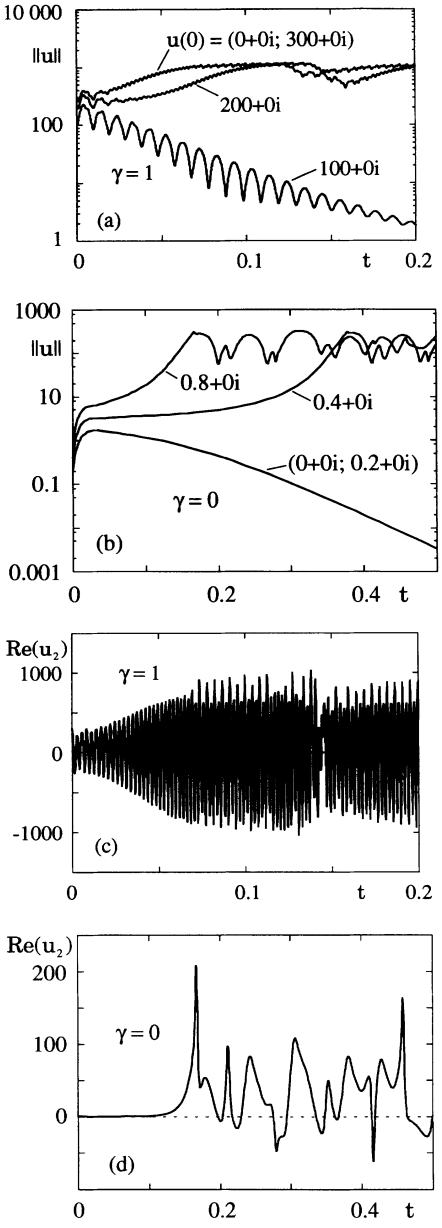

FIG. 5. (a) Perturbation amplitude $||\mathbf{u}(t)||$ for the model equation (1) and different initial vectors $\mathbf{u}(0) = [0 + 0i; 100 + 0i], [0 + 0i; 200 + 0i]$, and $[0 + 0i; 300 + 0i]$. The Reynolds number is $\mathcal{R} = 2000$ for the advective case. (b) Same as in (a), but for the nonadvective case. The initial vectors are $\mathbf{u}(0) = [0 + 0i; 0.2 + 0i], [0 + 0i; 0.4 + 0i]$, and $[0 + 0i; 0.8 + 0i]$ and the Reynolds number is $\mathcal{R} = 1000$. (c) Real part of u_2 for the initial vector $\mathbf{u}(0) = [0+0i; 300+0i]$ of (a). (d) Real part of u_2 for the initial vector $\mathbf{u}(0) = [0 + 0i; 0.8 + 0i]$ of (b).

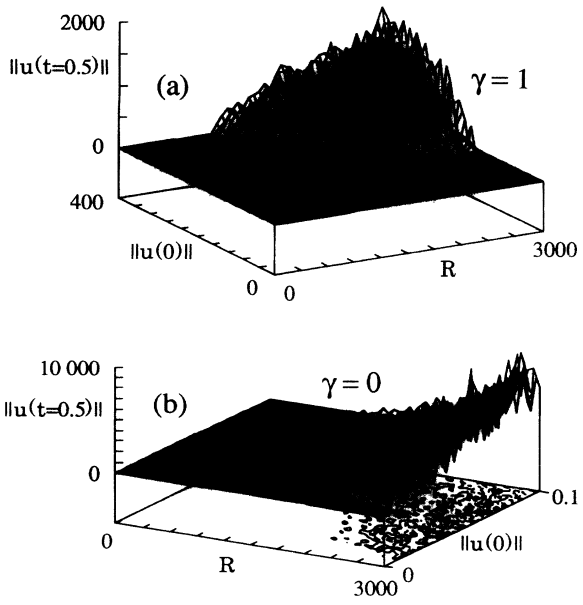

FIG. 6. (a) Perturbation amplitude at fixed time $t = 0.5$ as a function of the Reynolds number $\mathcal{R}$ and the initial amplitude $||\mathbf{u}(0)||$; $\gamma = 1$. (b) Same as in (a), but for $\gamma = 0$. The threshold of turbulence transition decreases roughly like $||\mathbf{u}(0)||_c \sim 1/\mathcal{R}$ for large $\mathcal{R}$. On the bottom plane the isolines of $||\mathbf{u}(t = 0.5)||$ =const are displayed.

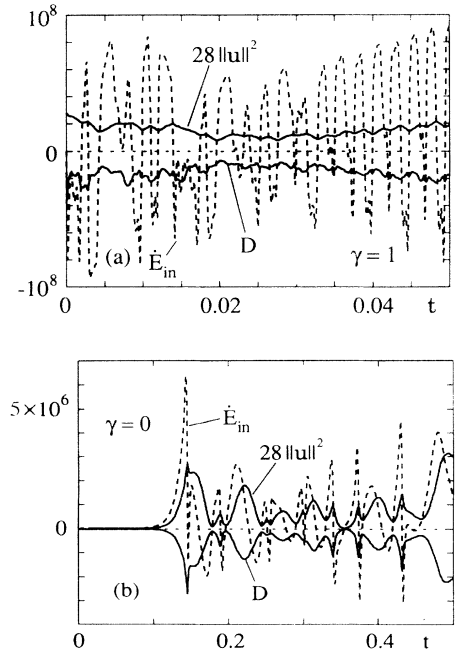

FIG. 7. Energy input $\dot{E}_{\text{in}}$ and dissipation D as a function of time. For comparison with the temporal evolution of the total energy $E = ||\mathbf{u}||^2/2$ we also plotted a constant multiple of E, namely, $28||\mathbf{u}||^2$. The prefactor 28 was chosen as the mean of the dissipation rates 18 and 38 to get a magnitude comparable to the dissipation D. We took the parameter γ and the initial value $\mathbf{u}(0)$ as in Figs. 4(a) and 4(b), respectively. The Reynolds numbers are (a) $\mathcal{R}$= 2000 and (b) $\mathcal{R}$= 1000.

We also investigated the influence of noise on the turbulence transition by adding to the variables after each time step of the integration routine a Gaussian random value with zero mean, variance s^2, and δ correlated in time. If that noise was strong enough it caused a transition away from the vicinity of the laminar state $\mathbf{u}(t = 0) = 0$. For the nonadvective case $\gamma = 0$ the noise level, which was necessary to induce turbulence, was rather low ($s \approx 2 \times 10^{-4}$) and did not change qualitatively the dynamics on the chaotic attractor. This was different for the advective case $\gamma = 1$, which needs a much larger s. We therefore focused our attention to the effect of noise on the nonadvective model, i.e., $\gamma = 0$. As expected, the two-component u_2 was much more susceptible to external noise than the one-component u_1, since with increasing $\mathcal{R}$ the second eigenvector becomes more and more parallel to the 1-direction and perpendicular to the 2-direction, so that disturbances in the 2-direction (represented by u_2) are misfit and grow transiently in the linearized system and can draw energy from the laminar background, respectively. As in the deterministic system the Reynolds number must be large enough to escape the laminar fixed point $\mathbf{u} = \mathbf{0}$ and to pass over to turbulence. Substituting the size of the initial perturbations $||\mathbf{u}(0)||$ of the deterministic system in Fig. 6 by the noise strength, we obtained a picture that was rather similar (Fig. 8).

Another feature that is independent of the detailed choice of the parameters is the asymptotic scaling of the turbulence energy. For large Reynolds numbers ($\mathcal{R} \gtrsim 8\,000$) the model (1) tends to be no longer chaotic, but to preferably exhibit limit cycles. This behavior is similar to that of the Lorenz system, which shows the same tendency if one chooses very large values for the driving parameter r. Again, in the asymptotic range of large Reynolds numbers $\mathcal{R}$ our model shows remarkable differences between $\gamma = 1$ and $\gamma = 0$. For the advective motion $\gamma = 1$ one has approximately $||\mathbf{u}|| \sim \mathcal{R}$ in the high-$\mathcal{R}$ regime and for $\gamma = 0$ one has $||\mathbf{u}|| \sim \mathcal{R}^2$ (cf. Fig. 9). This finding can be used for an estimate of the

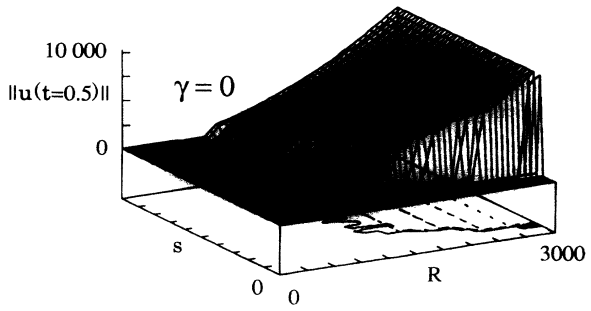

FIG. 8. Same as in Fig. 6(b), but driven by external noise. The initial vector is $||\mathbf{u}(0)|| = 0$. Here we used the standard fourth-order Runge-Kutta algorithm with constant time step size 5×10^{-6}. After each time step we added to each $\mathbf{u}$ component a random variable with Gaussian distribution and zero mean. The standard deviation s of this random variable was varied to model different noise levels. Its maximum value is about 5×10^{-4} in this figure.

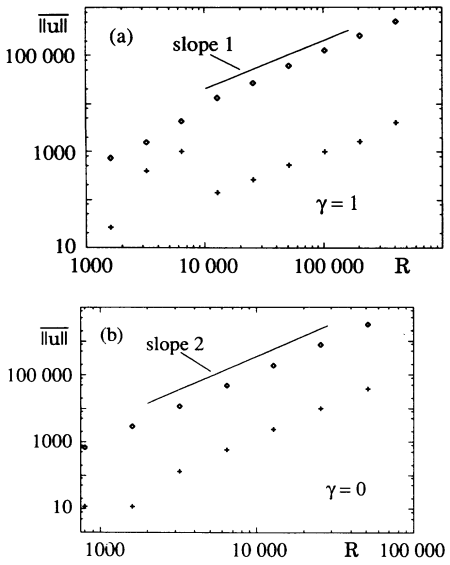

FIG. 9. Time averaged amplitude $\overline{||\mathbf{u}||}$ ($\diamond$) and its standard deviation (+) in the high-$\mathcal{R}$ regime. Each run is started with $\mathbf{u}(0) = (0 + 0i; 10^4 + 0i)$, averaging begins at $t = 0.1$, and the averaging interval is $\Delta t = 0.4$. As mentioned in the text, the attractor becomes a limit cycle for $\mathcal{R} \gtrsim 8000$, which shows up in a reduction of the standard deviation of $||\mathbf{u}||$ in comparison to that in the chaotic regime. The transition from a chaotic to a limit cycle attractor happens for smaller $\mathcal{R}$ in the nonadvective case $\gamma = 0$.

different terms of the right-hand side of (1). In the advective dynamics $\gamma = 1$ one has $\mathcal{R}(A_2 + C)\|\mathbf{u}\| \sim \mathcal{R}^2$ and also $B \sim \mathcal{R}^2$. Hence for large $\mathcal{R}$ the dynamics is controlled by an interplay of both contributions. In the nonadvective case $\gamma = 0$ one has $\mathcal{R}(A_2 + C)\mathbf{u} \sim \mathcal{R}^2$, but $B \sim \mathcal{R}^4$. Therefore the dynamics is essentially dominated by the nonlinear term.

V. SUMMARY

To sum up, our simple model qualitatively meets many features that can be observed in the turbulence transition of various flows that show no (or only very high $\mathcal{R}$) linear instability. The range of Reynolds numbers that is relevant for the transition is even quantitatively correct. The model suggests that the modes with large wavelengths in streamwise direction (corresponding to the nonadvective modes $\gamma = 0$) play a key role in this context since their capacity for energy amplification is most enhanced. But also modes with shorter wavelengths can contribute to the dynamics when they are excited beyond a certain threshold. In hydrodynamic flow the large wavelength modes might well act via the nonlinear interactions as such an above threshold perturbation on the short-wavelength modes. So the actual dynamics of turbulence without linear instability takes place in a very high dimensional phase space.

This new route to chaos and its dependence on the system parameters, which in our model are the Reynolds number $\mathcal{R}$ and the missing or relevant difference of the imaginary parts of the eigenvalues ($\gamma = 0$ or $\gamma = 1$, respectively), may be important in many other situations too, namely, whenever linear stability coincides with nonnormality of the linear dynamics together with proper remixing by the nonlinear interactions.

Note added in proof. After submitting our paper we became aware of a manuscript by F. Waleffe (unpublished). This author also considers a model with four real variables, which has many features similar to our model (1), but with a different meaning of the four variables. Those are intended to describe the structure of the flow field, which is supposed to be responsible for the amplification of the disturbances. There also a switch-off for the mean shear, which is an important part of our model, is included (by a separate equation of motion).

ACKNOWLEDGMENTS

This work was supported by the Deutsche Forschungsgemeinschaft via the SFB 185 (Nichtlineare Dynamik — Instabilitäten und Strukturbildung in Physikalischen Systemen). We thank Detlef Lohse for very helpful remarks.

[1] L. Boberg and U. Brosa, Z. Naturforsch. **43a**, 697 (1988).
[2] S. Reddy and D. Henningson, J. Fluid Mech. **252**, 209 (1993).
[3] B. Farrel and P. Ioannou, Phys. Fluids A **5**, 2298 (1993).
[4] L. Trefethen, A. Trefethen, S. Reddy, and T. Driscol, Science **261**, 578 (1993).
[5] D. Henningson and S. Reddy, Phys. Fluids **6**, 1396 (1994).
[6] C. Doering and P. Constantin, Phys. Rev. Lett. **69**, 1648 (1992).
[7] B. Farrel and P. Ioannou, Phys. Rev. Lett. **72**, 1188 (1994).
[8] We generally used the Bulirsch-Stoer algorithm with adaptive step size to integrate the ODE's.

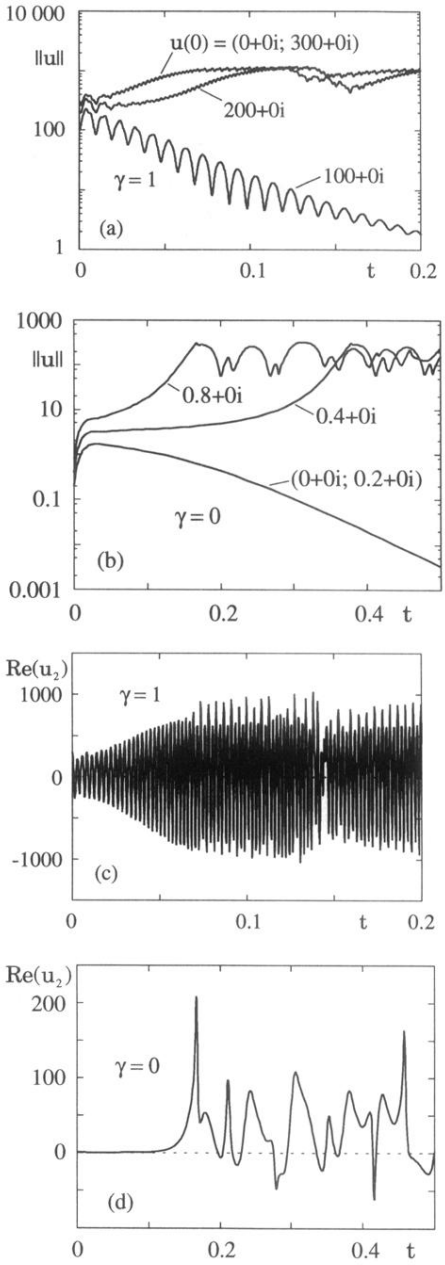

FIG. 5. (a) Perturbation amplitude $||\mathbf{u}(t)||$ for the model equation (1) and different initial vectors $\mathbf{u}(0) = [0 + 0i; 100 + 0i], [0 + 0i; 200 + 0i]$, and $[0 + 0i; 300 + 0i]$. The Reynolds number is $\mathcal{R} = 2000$ for the advective case. (b) Same as in (a), but for the nonadvective case. The initial vectors are $\mathbf{u}(0) = [0 + 0i; 0.2 + 0i], [0 + 0i; 0.4 + 0i]$, and $[0 + 0i; 0.8 + 0i]$ and the Reynolds number is $\mathcal{R} = 1000$. (c) Real part of u_2 for the initial vector $\mathbf{u}(0) = [0+0i; 300+0i]$ of (a). (d) Real part of u_2 for the initial vector $\mathbf{u}(0) = [0 + 0i; 0.8 + 0i]$ of (b).

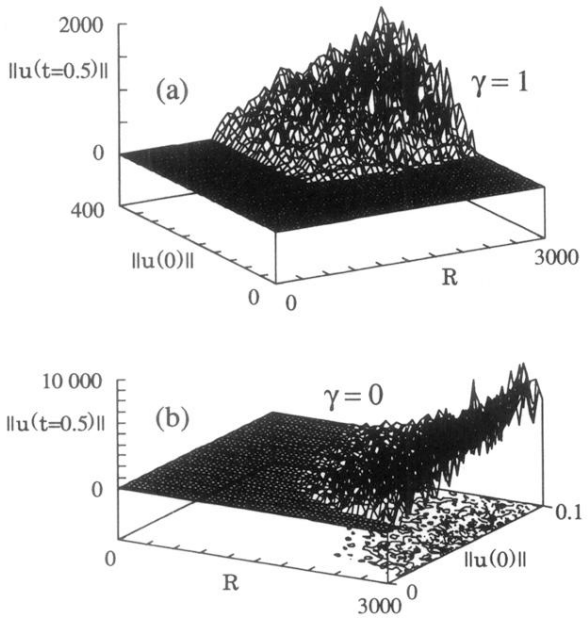

FIG. 6. (a) Perturbation amplitude at fixed time $t = 0.5$ as a function of the Reynolds number $\mathcal{R}$ and the initial amplitude $||\mathbf{u}(0)||$; $\gamma = 1$. (b) Same as in (a), but for $\gamma = 0$. The threshold of turbulence transition decreases roughly like $||\mathbf{u}(0)||_c \sim 1/\mathcal{R}$ for large $\mathcal{R}$. On the bottom plane the isolines of $||\mathbf{u}(t = 0.5)||$ =const are displayed.

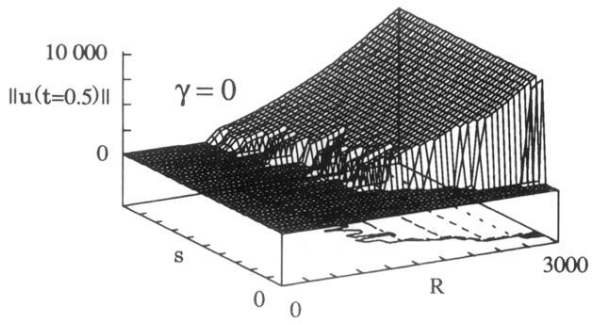

FIG. 8. Same as in Fig. 6(b), but driven by external noise. The initial vector is $||\mathbf{u}(0)|| = 0$. Here we used the standard fourth-order Runge-Kutta algorithm with constant time step size 5×10^{-6}. After each time step we added to each $\mathbf{u}$ component a random variable with Gaussian distribution and zero mean. The standard deviation s of this random variable was varied to model different noise levels. Its maximum value is about 5×10^{-4} in this figure.